Electronic Supplementary Information

Facile and sustainable synthesis of sodium lignosulfonate derived hierarchical porous carbons for supercapacitors with high volumetric energy density

Jie Pang [a, c], Wenfeng Zhang [b, c, *], Jinliang Zhang [a, c], Gaoping Cao [b, c], Minfang Han [a], Yusheng Yang [b, c]

a. School of Chemical and Environmental Engineering, China University of Mining and Technology (Beijing), Beijing 100083, China.
b. Research Institute of Chemical Defense, Beijing 100191, China. E-mail: wenfengzh@163.com
c. Beijing Key Laboratory of Advanced Chemical Energy Storage Technology and Materials, Beijing 100191, China.

S1 Electrochemical measurements

The gravimetric (C_g, F g^{-1}), volumetric (C_v, F cm^{-3}) and areal (C_a, μF cm^{-2}) specific capacitance of a single electrode was calculated from the discharge curves according to the following equations:[1, 2]

$$C_g = \frac{2I\Delta t}{m\Delta V} \quad (1)$$

$$C_v = C_g \rho \quad (2)$$

$$\rho = \frac{1}{V_{total} + (1/\rho_{carbon})} \quad (3)$$

$$C_a = \frac{100 \times C_g}{S_{BET}} \quad (4)$$

where I (A) is the constant discharge current, Δt (s) is the discharge time, m (g) is the mass of the active material in a single electrode, ΔV (V) is the potential change in discharge, ρ (g cm^{-3}) is the particle density of the carbon sample, V_{total} (cm^3 g^{-1}) is the total pore volume of the carbon sample measured by N_2 isotherms, ρ_{carbon} (2 g cm^{-3}) is the true density of carbon, and S_{BET} (m^2 g^{-1}) is the specific surface area of the carbon sample obtained from the BET method.

The gravimetric/volumetric energy density (E_g, Wh kg^{-1}; E_v, Wh L^{-1}) and power density (P_g, W kg^{-1}; P_v, W L^{-1}) of the two-electrode symmetric supercapacitors were also calculated according to equation (5 – 8):

$$E_g = \frac{C_g \Delta V^2}{8 \times 3.6} \quad (5)$$

$$P_g = \frac{3600 \times E_g}{\Delta t} \quad (6)$$

$$E_v = E_g \rho \quad (7)$$

$$P_v = P_g \rho \quad (8)$$

where C_g (F g^{-1}) represents the gravimetric specific capacitance of a single electrode obtained from equation (1), ΔV (V) is the potential change in discharge, Δt (s) is the discharge time, and ρ (g cm^{-3}) is the particle density of the carbon sample.

Table S1 Elemental analysis of SLS from EDS and ICP-AES.

Sample	EDS								ICP-AES			
	Nonmetal element (wt.%)				Metal element (wt.%)				Metal element (wt.%)			
	C	O	S	Cl	Na	K	Mg	Ca	Na	K	Mg	Ca
SLS	41.85	42.04	4.17	1.33	9.01	1.38	-	-	13.35	3.23	0.07	0.24

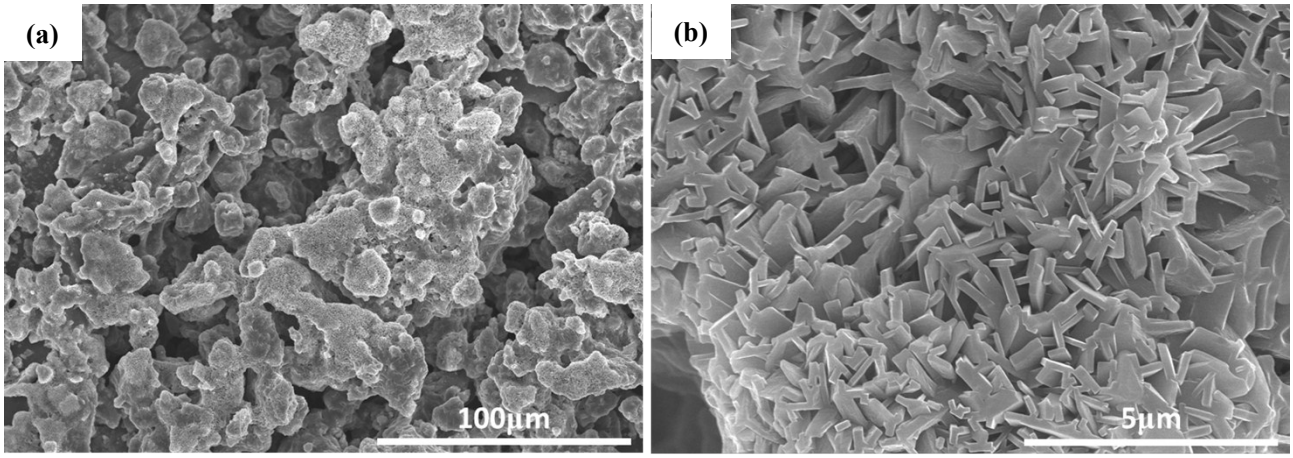

Fig. S1 (a-b) SEM images at different magnifications of the product by carbonization of SLS at 800 ℃ for 1h (before washing).

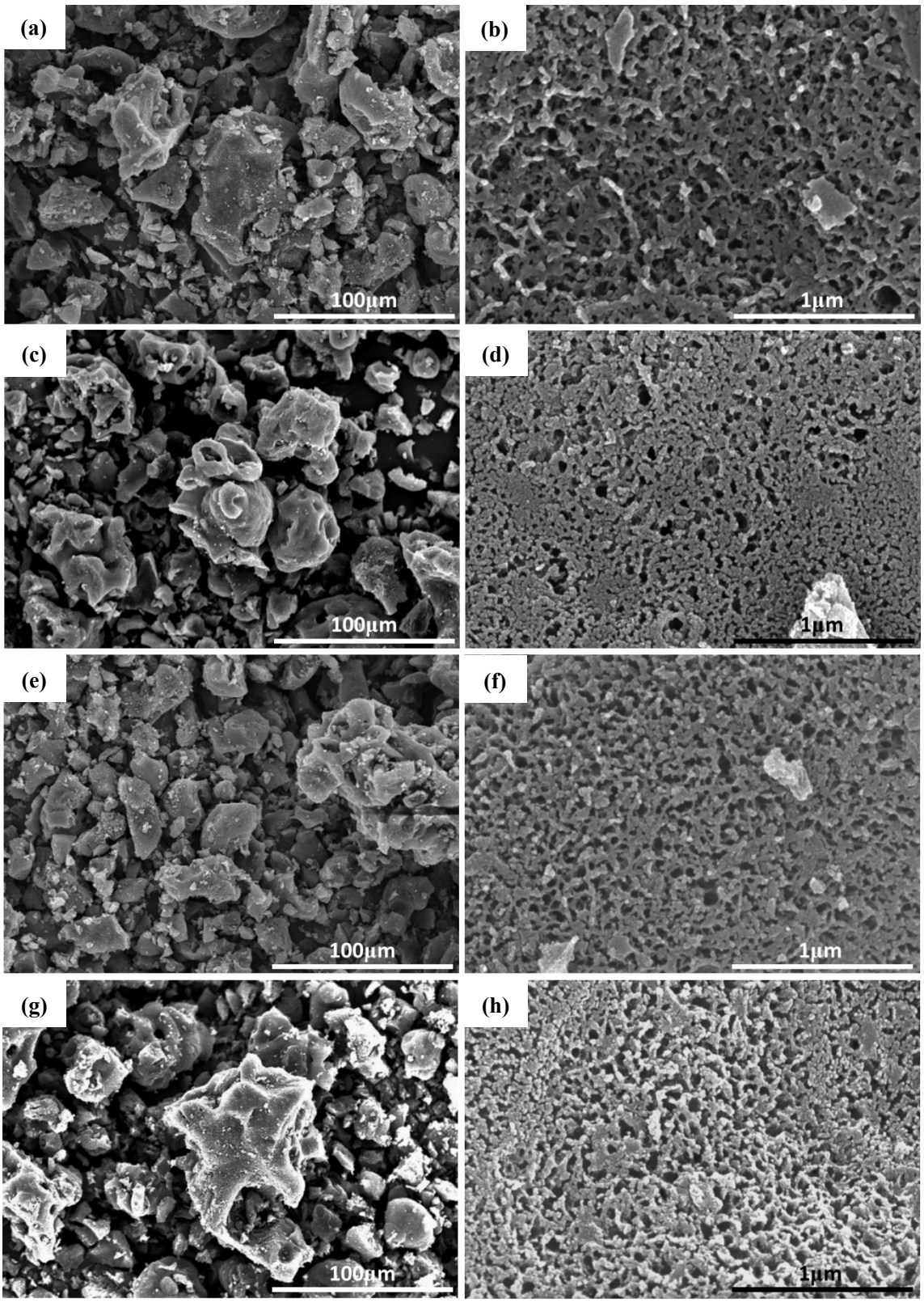

Fig. S2 SEM images of (a-b) HPCSLS-600-1, (c-d) HPCSLS-700-1, (e-f) HPCSLS-900-1 and (g-h) HPCSLS-1000-1 at different magnifications.

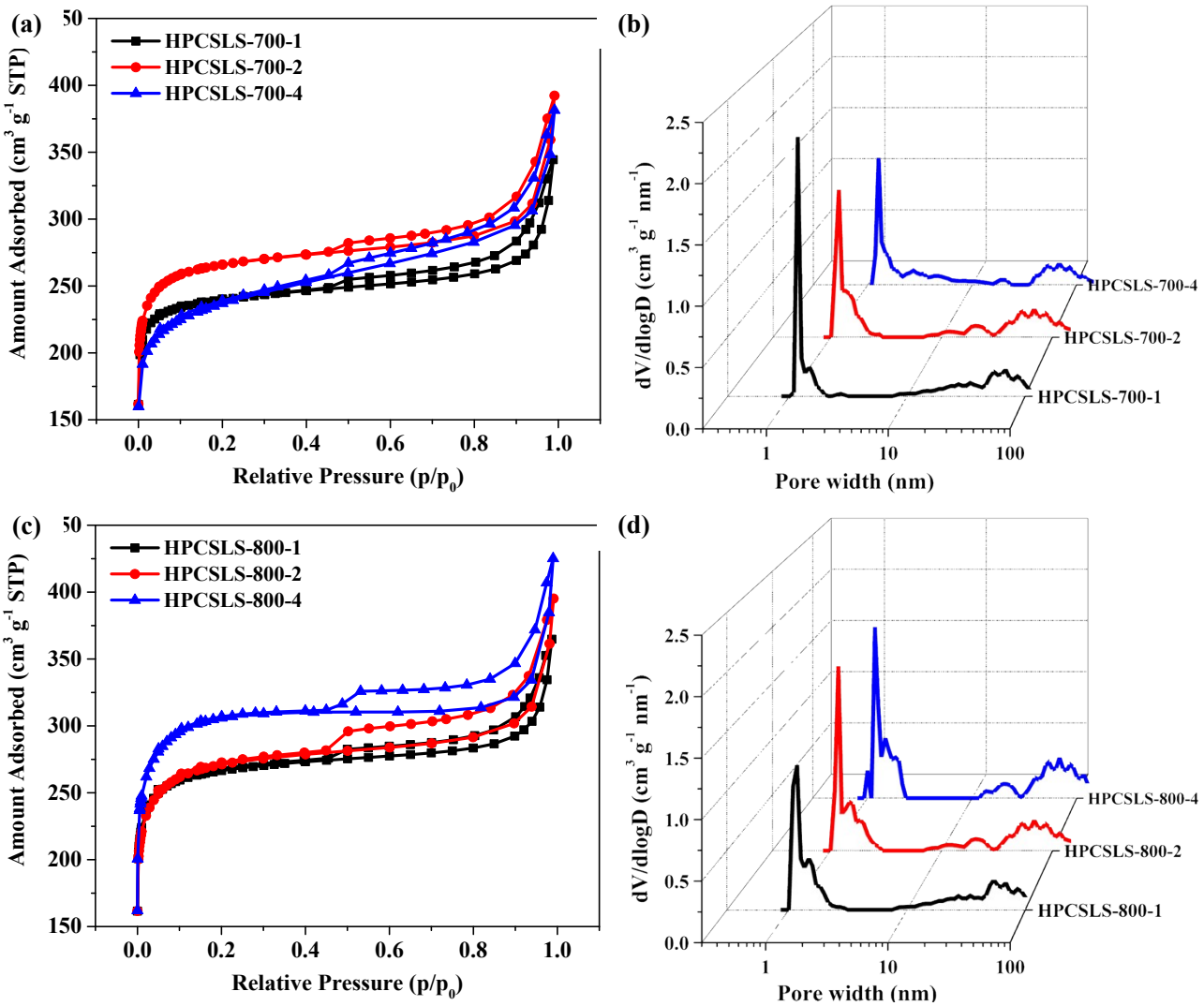

Fig. S3 (a) Nitrogen adsorption-desorption isotherms and (b) DFT pore size distributions of the HPCSLS-700-Y samples. (c) Nitrogen adsorption-desorption isotherms and (d) DFT pore size distributions of the HPCSLS-800-Y samples.

Table S2 Textural properties, surface elemental contents and electrochemical performances of HPCSLS-700-Y and HPCSLS-800-Y.

Sample	N_2 adsorption-desorption						XPS				C_g[g]	C_v[g]	C_a[g]
	SSA (m^2 g^{-1})			Pore volume (cm^3 g^{-1})			Elemental content (at.%)				(F g^{-1})	(F cm^{-3})	(μF cm^{-2})
	S_{BET}[a]	S_{micro}[b]	S_{ext}[c]	V_{total}[d]	V_{micro}[e]	V_{meso}[f]	C	N	O	S			
HPCSLS-700-2	1006	832	174	0.61	0.33	0.06	92.04	1.60	6.10	0.26	201	181	20.0
HPCSLS-700-4	884	610	274	0.59	0.26	0.08	92.63	1.32	5.80	0.24	172	158	19.5
HPCSLS-800-2	1028	805	223	0.61	0.33	0.07	91.71	0.99	7.05	0.26	161	145	15.7
HPCSLS-800-4	1164	921	244	0.66	0.39	0.08	93.59	0.87	5.32	0.21	149	128	12.8

a: Specific surface area (S_{BET}) calculated by BET method.

b, c: Specific micropore area (S_{micro}) and specific external surface area (S_{ext}) calculated by t-plot method.

d: Total pore volume (V_{total}) determined at a relative pressure (P/P_0) of 0.97.

e, f: Micropore volume (V_{micro}) and mesopore volume (V_{meso}) calculated by DFT model.

g: The C_g, C_v and C_a values calculated from discharge curves at a current density of 0.05 A g^{-1}.

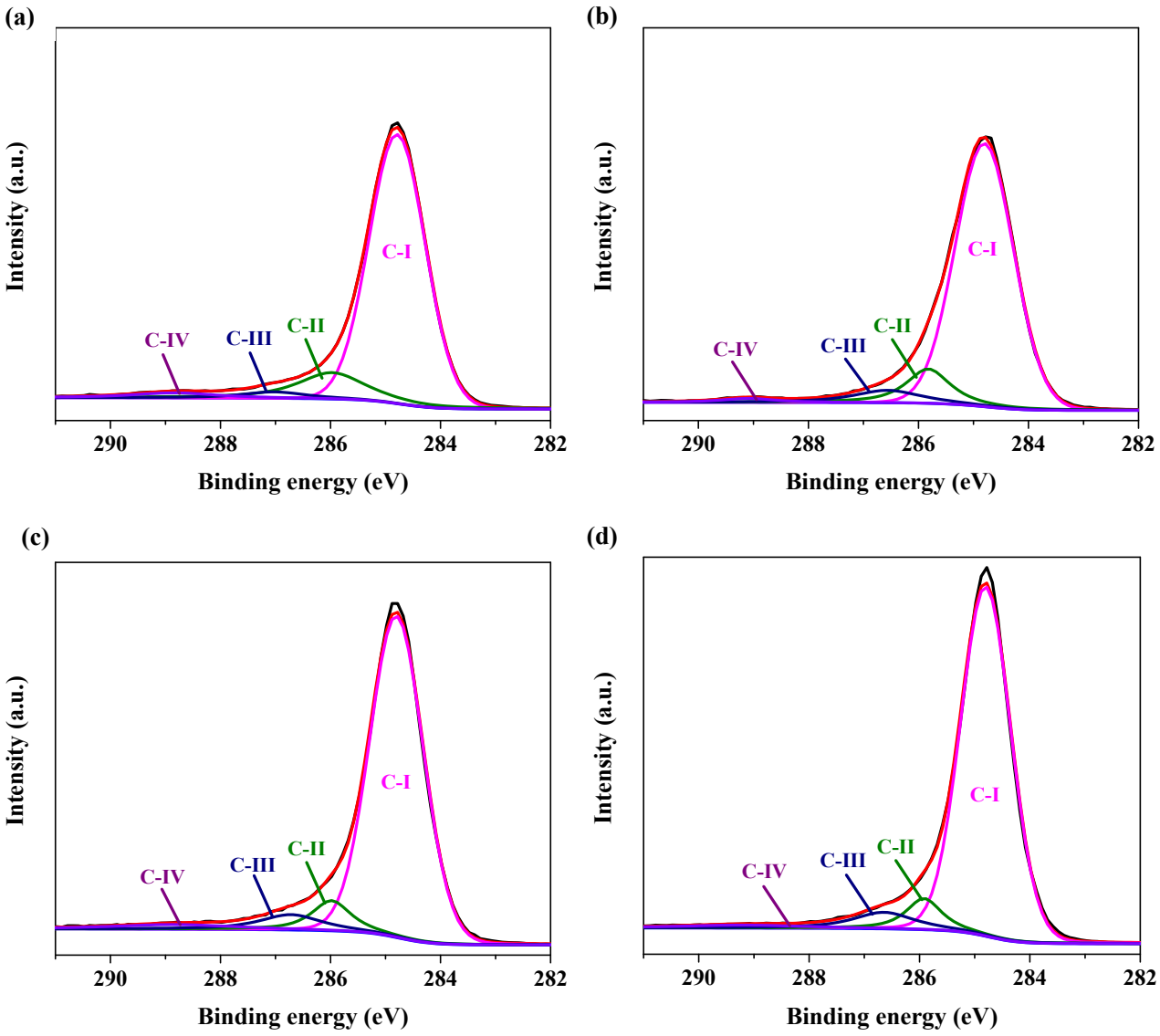

Fig. S4 C 1s XPS spectra of (a) HPCSLS-600-1, (b) HPCSLS-800-1, (c) HPCSLS-900-1 and (d) HPCSLS-1000-1.

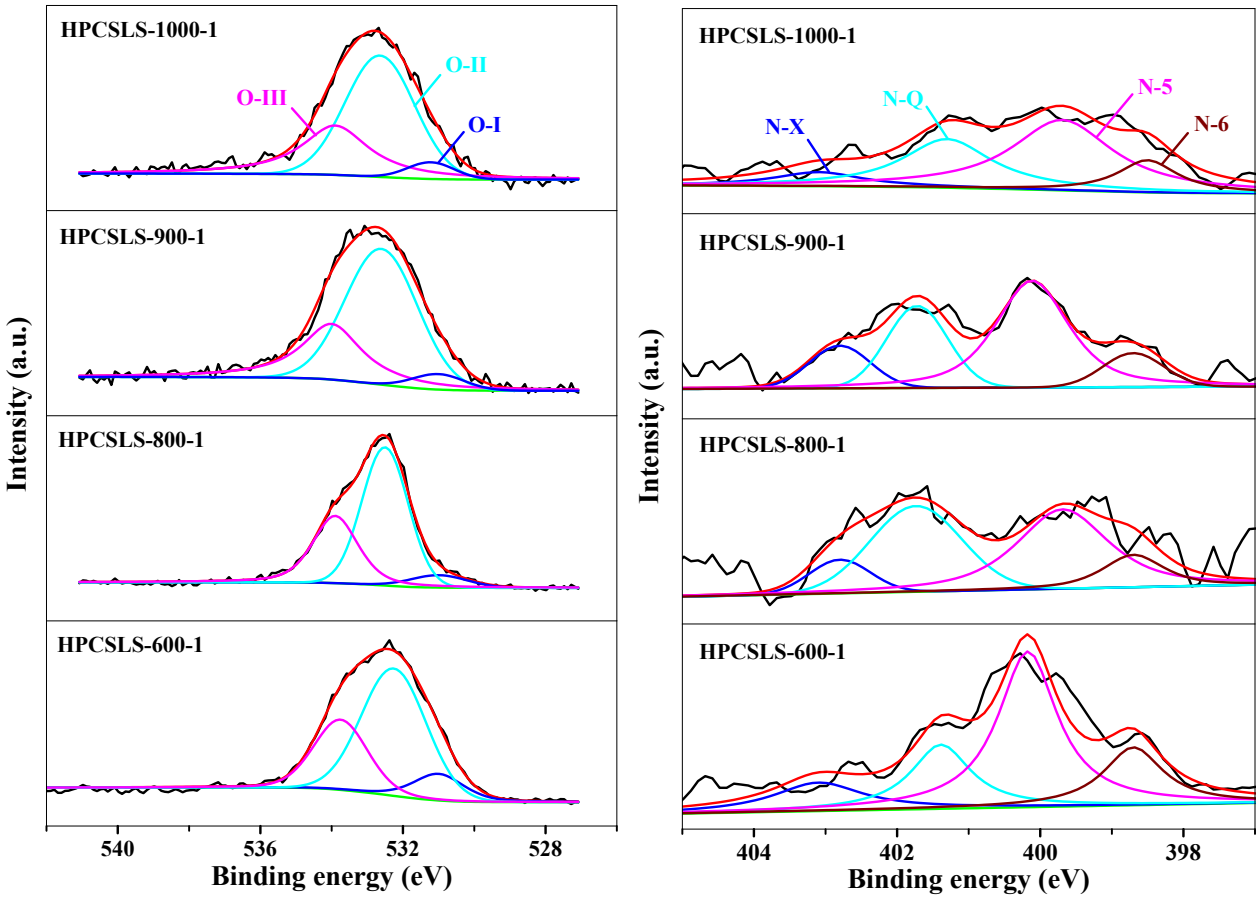

Fig. S5 (a) O 1s and (b) N 1s XPS spectra of the HPCSLS-X-1 samples.

Table S3 Surface C, O and N configurations of HPCSLS-X-1 by XPS.

Sample	C configuration[a] (at.%)				O configuration[b] (at.%)			N configuration[c] (at.%)			
	C-I	C-II	C-III	C-IV	O-I	O-II	O-III	N-6	N-5	N-Q	N-X
HPCSLS-600-1	80.68	13.14	3.01	3.17	11.45	59.25	29.30	18.05	48.58	20.04	13.33
HPCSLS-700-1	81.09	10.04	6.04	2.83	8.45	58.76	32.79	22.48	38.08	26.03	13.41
HPCSLS-800-1	81.40	10.91	6.13	1.56	6.52	59.36	34.12	11.76	43.46	35.49	9.29
HPCSLS-900-1	82.38	7.65	6.20	3.77	5.14	62.82	32.04	10.47	51.12	25.28	13.13
HPCSLS-1000-1	83.80	7.16	6.54	2.49	5.54	59.52	34.94	13.10	48.67	29.65	8.58

a: C sp^2 and sp^3 (C-I), C−O (C-II), C=O (C-III) and O−C=O (C-IV).

b: C=O (O-I), C−OH and/or C−O−C (O-II), −COOH (O-III).

c: Pyridinic nitrogen (N-6), pyrrolic nitrogen (N-5), quaternary-N (N-Q), N-oxides group (N-X).

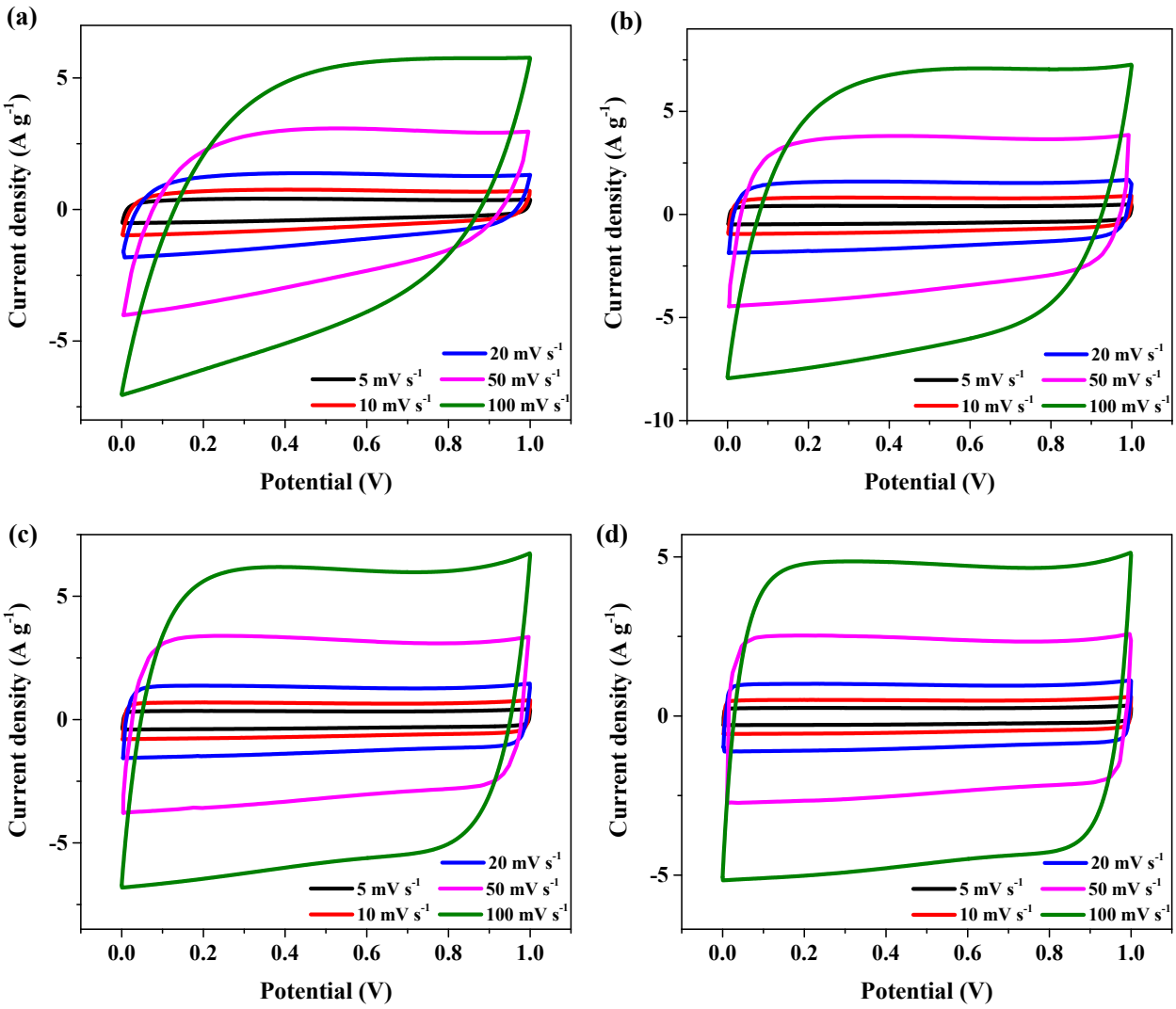

Fig. S6 CV curves tested at 5 – 100 mV s^{-1} of (a) HPCSLS-600-1, (b) HPCSLS-800-1, (c) HPCSLS-900-1 and (d) HPCSLS-1000-1.

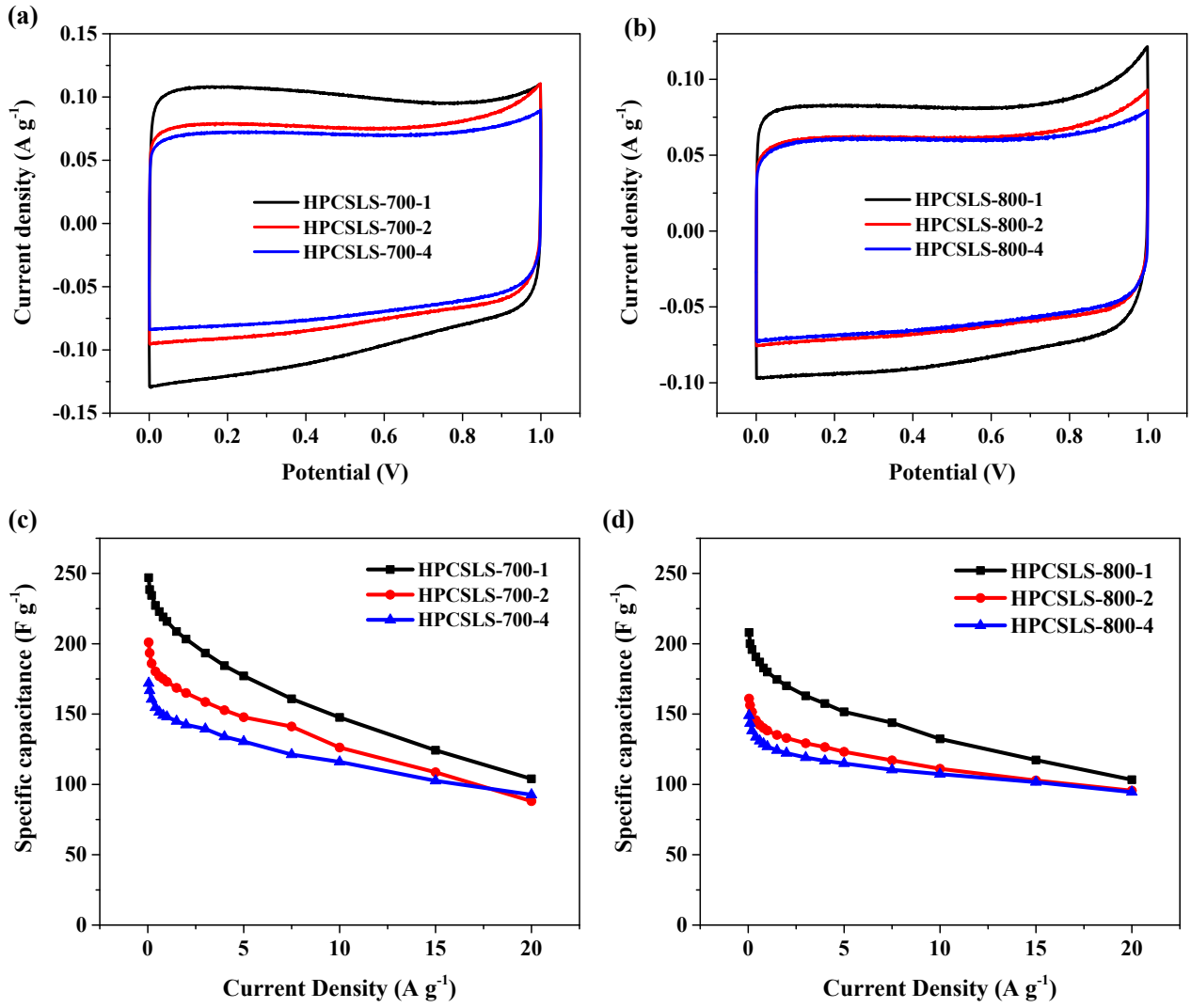

Fig. S7 CV curves tested at a scan rate of 1 mV s^{-1} of (a) HPCSLS-700-Y and (b) HPCSLS-800-Y. Charge-discharge rate performance of (c) HPCSLS-700-Y and (d) HPCSLS-800-Y.

Table S4 Equivalent series resistance (ESR), charge transfer resistance (R_{ct}), and diffusion resistance (R_d) of HPCSLS-X-1 obtained from the equivalent circuit model fitting.

Sample	Resistance (Ω)		
	R_{esr}	R_{ct}	R_d
HPCSLS-600-1	1.323	0.403	0.722
HPCSLS-700-1	1.042	0.226	0.692
HPCSLS-800-1	0.681	0.081	0.659
HPCSLS-900-1	0.605	0.063	0.529
HPCSLS-1000-1	0.469	0.030	0.420

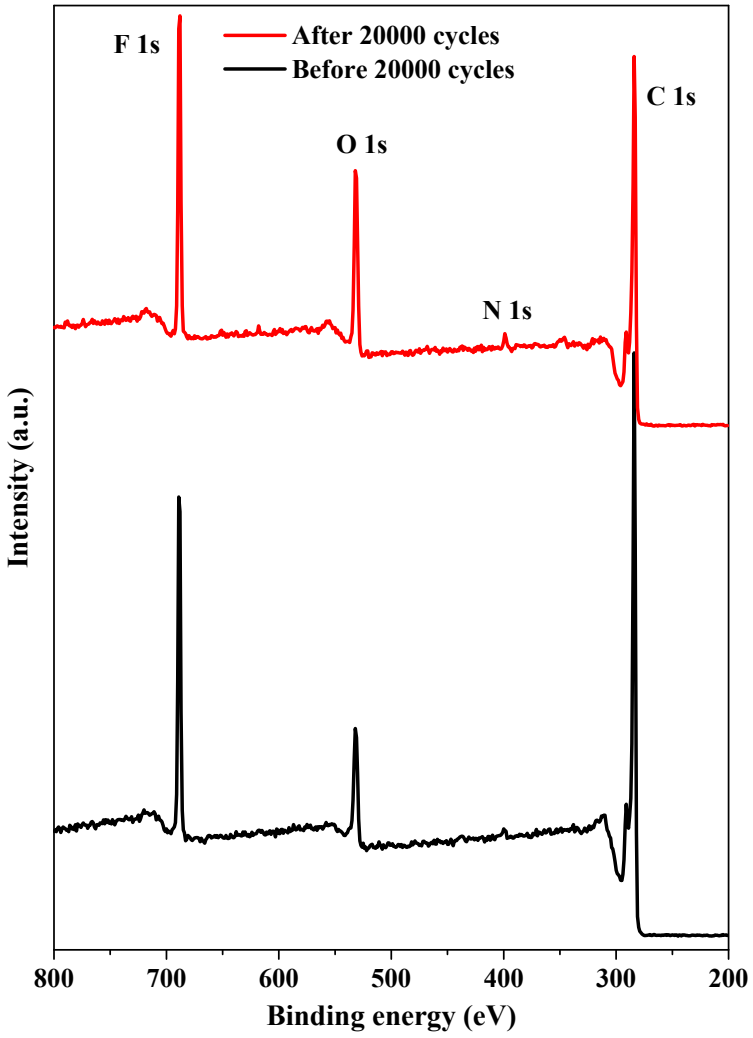

Fig. S8 XPS spectra of HPCSLS-700-1 based electrodes before and after long-term cycling test.

Table S5 Performance comparison of lignin/biomass based porous carbons for supercapacitor application reported in the literatures.

Precursor	Preparation	Electrolyte	Test condition	C_g ($F\ g^{-1}$)	C_v ($F\ cm^{-3}$)	C_a ($\mu F\ cm^{-2}$)	Refs.
Lignin	Hard templating + electro-oxidation	1 M H_2SO_4	0.05 A g^{-1}	249	149	29	3
Lignin	Physical activation	1 M H_2SO_4	10 mV s^{-1}	201	214	20.0	4
Lignin	Hard-soft templating	6 M KOH	0.1 A g^{-1}	208.4	153.2	26.0	5
Lignin	Chemical activation	6 M KOH	0.5 A g^{-1}	268	205	18.6	6
Kraft lignin	Soft templating + physical activation	6 M KOH	1 mV s^{-1}	102.3	83.2	16.4	7
Kraft lignin	Without activation and templating	1 M H_2SO_4	0.5 A g^{-1}	91	NA	8.3	8
Alkali lignin	Polymer blending	6 M KOH	0.4 A g^{-1}	64	81	11	9
Alkali lignin	Chemical activation	1 M H_2SO_4	0.05 A g^{-1}	165.0	162.6	18.2	10
Alkali lignin	Chemical activation	6 M KOH	0.2 A g^{-1}	286.7	89.5	7.6	11
Alkali lignin	Chemical activation	6 M KOH	10 mV s^{-1}	240	-	17.1	12
Solvent lignin	Chemical activation + N-doped	6 M KOH	0.1 A g^{-1}	248	NA	11.0	13
Solvent lignin	Chemical activation + N-doped	6 M KOH	20 mV s^{-1}	333	NA	14.7	14
Solvent lignin	Chemical activation + N-doped	6 M KOH	0.1 A g^{-1}	273	126	8.7	15
Lignin-derived byproduct	Chemical activation	6 M KOH	1 A g^{-1}	312	NA	14.1	16
Calcium lignosulfonate	Without activation and templating	6 M KOH	1 mA cm^{-2}	182	137	13.4	17
Lignosulfonate	Hard templating + chemical activation	6 M KOH	0.25 A g^{-1}	286	265	33.4	18
Fruit stone	Chemical activation + P-doped	1 M H_2SO_4	0.05 A g^{-1}	131	112	10.4	19
Wood sawdust	Chemical activation	6 M KOH	0.5 A g^{-1}	225	118	9.8	20
Shells of broad beans	Chemical activation + N, S dual doped	6 M KOH	0.5 A g^{-1}	202	229	30.8	21
Cashmere	Chemical activation + N, O dual doped	6 M KOH	0.5 A g^{-1}	144	83	10.6	22
Cellulose	Chemical activation	6 M KOH	0.1 A g^{-1}	253	135	13.4	23
Loblolly pine	Chemical activation	6 M KOH	20 mV s^{-1}	74	80	7.7	24
Waste Coca Cola®	Chemical activation + O, N, S co-doped	6 M KOH	1 A g^{-1}	352.7	256.9	17.7	25
Rice straw	Chemical activation	6 M KOH	0.5 A g^{-1}	269	151	10.2	26
Cattail biomass	Physical activation	6 M KOH	0.5 A g^{-1}	126.5	152.4	28.7	27
Sodium lignosulfonate (HPCSLS-700-1)	Without activation and templating	7 M KOH	0.05 A g^{-1}	247	240	27.4	This work
			0.4 A g^{-1}	227	220	25.1	

References

1. J. W. Lang, X. B. Yan, W. W. Liu, R. T. Wang and Q. J. Xue, *J. Power Sources*, 2012, **204**, 220-229.
2. J. Hou, C. Cao, X. Ma, F. Idrees, B. Xu, X. Hao and W. Lin, *Sci. Rep.*, 2014, **4**, 1-6.
3. R. Ruiz-Rosas, M. J. Valero-Romero, D. Salinas-Torres, J. Rodriguez-Mirasol, T. Cordero, E. Morallon and D. Cazorla-Amoros, *ChemSusChem*, 2014, **7**, 1458-1467.
4. R. Berenguer, F. J. Garcia-Mateos, R. Ruiz-Rosas, D. Cazorla-Amoros, E. Morallon, J. Rodriguez-Mirasol and T. Cordero, *Green Chem.*, 2016, **18**, 1506-1515.
5. H. Li, D. Yuan, C. Tang, S. Wang, J. Sun, Z. Li, T. Tang, F. Wang, H. Gong and C. He, *Carbon*, 2016, **100**, 151-157.
6. Z.-z. Chang, B.-j. Yu and C.-y. Wang, *J. Solid State Electrochem.*, 2016, **20**, 1405-1412.
7. D. Saha, Y. Li, Z. Bi, J. Chen, J. K. Keum, D. K. Hensley, H. A. Grappe, H. M. Meyer, III, S. Dai, M. P. Paranthaman and A. K. Naskar, *Langmuir*, 2014, **30**, 900-910.
8. J. W. Jeon, L. Zhang, J. L. Lutkenhaus, D. D. Laskar, J. P. Lemmon, D. Choi, M. I. Nandasiri, A. Hashmi, J. Xu, R. K. Motkuri, C. A. Fernandez, J. Liu, M. P. Tucker, P. B. McGrail, B. Yang and S. K. Nune, *ChemSusChem*, 2015, **8**, 428-432.
9. C. Lai, Z. Zhou, L. Zhang, X. Wang, Q. Zhou, Y. Zhao, Y. Wang, X. F. Wu, Z. Zhu and H. Fong, *J. Power Sources*, 2014, **247**, 134-141.
10. W. Zhang, H. Lin, Z. Lin, J. Yin, H. Lu, D. Liu and M. Zhao, *ChemSusChem*, 2015, **8**, 2114-2122.
11. W. Zhang, M. Zhao, R. Liu, X. Wang and H. Lin, *Colloids Surf. A Physicochem. Eng. Asp.*, 2015, **484**, 518-527.
12. S. Hu, S. Zhang, N. Pan and Y.-L. Hsieh, *J. Power Sources*, 2014, **270**, 106-112.
13. K. Wang, Y. Cao, Z. Gu, P. Ahrenkiel, J. Lee and Q. H. Fan, *RSC Adv.*, 2016, **6**, 26738-26744.
14. K. Wang, Y. Cao, X. Wang, M. A. Castro, B. Luo, Z. Gu, J. Liu, J. D. Hoefelmeyer and Q. Fan, *J. Power Sources*, 2016, **307**, 462-467.
15. K. Wang, M. Xu, Y. Gu, Z. Gu and Q. H. Fan, *J. Power Sources*, 2016, **332**, 180-186.
16. L. Zhang, T. You, T. Zhou, X. Zhou and F. Xu, *ACS Appl. Mater. Inter.*, 2016, **8**, 13918-13925.
17. X. Y. Chen and Q. Q. Zhou, *Electrochim. Acta*, 2012, **71**, 92-99.
18. Z. Zhao, S. Hao, P. Hao, Y. Sang, A. Manivannan, N. Wu and H. Liu, *J. Mater. Chem. A*, 2015, **3**, 15049-15056.
19. C. Huang, A. M. Puziy, T. Sun, O. I. Poddubnaya, F. Suarez-Garcia, J. M. D. Tascon and D. Hulicova-Jurcakova, *Electrochim. Acta*, 2014, **137**, 219-227.
20. Y. Huang, L. Peng, Y. Liu, G. Zhao, J. Y. Chen and G. Yu, *ACS Appl. Mater. Inter.,* 2016, **8**, 15205-15215.
21. G. Xu, J. Han, B. Ding, P. Nie, J. Pan, H. Dou, H. Li and X. Zhang, *Green Chem.*, 2015, **17**, 1668-1674.
22. L. Zhou, H. Cao, S. Zhu, L. Hou and C. Yuan, *Green Chem.*, 2015, **17**, 2373-2382.
23. J. Deng, T. Xiong, F. Xu, M. Li, C. Han, Y. Gong, H. Wang and Y. Wang, *Green Chem.*, 2015, **17**, 4053-4060.
24. N. He, S. Yoo, J. Meng, O. Yildiz, P. D. Bradford, S. Park and W. Gao, *Carbon*, 2017, **120**, 304-312.
25. Y. Boyjoo, Y. Cheng, H. Zhong, H. Tian, J. Pan, V. K. Pareek, S. P. Jiang, J.-F. Lamonier, M. Jaroniec and J. Liu, *Carbon*, 2017, **116**, 490-499.
26. L. Zhu, F. Shen, R. L. Smith, Jr., L. Yan, L. Li and X. Qi, *Chem. Eng. J.*, 2017, **316**, 770-777.
27. M. Yu, Y. Han, J. Li and L. Wang, *Chem. Eng. J.*, 2017, **317**, 493-502.